Flux Analysis in Process Models via Causality

Ozan Kahramanoğulları
The Microsoft Research – University of Trento
Centre for Computational and Systems Biology

We present an approach for flux analysis in process algebra models of biological systems. We perceive flux as the flow of resources in stochastic simulations. We resort to an established correspondence between event structures, a broadly recognised model of concurrency, and state transitions of process models, seen as Petri nets. We show that we can this way extract the causal resource dependencies in simulations between individual state transitions as partial orders of events. We propose transformations on the partial orders that provide means for further analysis, and introduce a software tool, which implements these ideas. By means of an example of a published model of the Rho GTP-binding proteins, we argue that this approach can provide the substitute for flux analysis techniques on ordinary differential equation models within the stochastic setting of process algebras.

1 Introduction

Computer science methodologies are now gaining increasing attention in systems biology, where they are used together with techniques from applied mathematics and physics to provide insights into the workings of biological systems. In such a setting, it is often desirable to model smaller biological systems as sets of differential equations. Being equipped with well understood analysis techniques, differential equations provide the deterministic approach (as opposed to the stochastic approach) for modelling and simulating biological systems. Differential equation models, however, are inherently difficult to change, extend and upgrade when modification to the model structure is required. In addition, within the last few years, a general consensus has emerged that noise and stochastic effects, which are not directly captured by differential equations, are essential attributes of biological systems (see, e.g., [25]).

'Tailored to fit' constructs of computer science languages provide the means for building models of larger systems, especially when it is required to refine, modify or compose the models, for example when new data is acquired. Various languages with stochastic simulation capabilities based on, for example, process algebras [24, 6, 15, 23], term rewriting (see, e.g, [9, 13]) and Petri nets (see, e.g., [16, 26]) have been proposed. In particular, process algebras, which were originally introduced to study the properties of complex, reactive, concurrent systems are well suited for modelling biological systems. By using these languages, we can build models to describe the dynamics of the biological systems, which are inherently complex and massively parallel, and run stochastic simulations. The time series data resulting from these stochastic simulations are then used to observe the emergent behaviour, together with other techniques that are borrowed from theoretical computer science to explore the model for hypothesis generation. However, these techniques are still underdeveloped in comparison to the rich arsenal of differential equation analysis techniques that have their roots in Newton's physics. There is now a pressing need for the adjustment of the computer science analysis techniques on models of biological systems and on stochastic simulations with them so that biologically meaningful observations can be made.

Along these lines, we present an approach for the analysis of stochastic simulations with process algebra models. The stochastic semantics of process algebras are conveniently given by continuous time

E. Merelli and P. Quaglia (Eds.)
From Biology To Concurrency and back 2010 (FBTC'10)
EPTCS 19, 2010, pp. 20–39, doi:10.4204/EPTCS.19.2

© Kahramanoğulları
This work is licensed under the
Creative Commons Attribution License.

Markov chains (CTMC). Each simulation is a trajectory of a CTMC, which is a sequence of computations of the underlying transition system, given by the process algebra model. The CTMC semantics, thus, imposes a total order on the transitions of a simulation trajectory that is emphasised by the unique time stamps of the individual transitions. In this respect, a simulation on a model can be seen as reduction of a complex structure, i.e., the model, into a simpler structure, i.e., the simulation trajectory. However, during this reduction some of the information on the model is lost, and others are made implicit. The idea here is to recover this implicit information: when these transitions are inspected from the point of view of their dependencies on one another, it is possible to relax the total order of the transitions into a partial order. We can then use this partial order as a representation of causal dependencies in the simulation and process it to observe the flux in the system with respect to the flow of the resources during simulation from one transition to another.

Partial orders reflecting dependencies in computations have been studied as non-interleaving models of concurrency: when there are no resource conflicts between two partially ordered events, they can take place in parallel, and their common predecessors and successors provide a synchronisation mechanism. Event structures reflect this view [21, 27]: in an event structure dependencies of events of a concurrent system are given with a partial order. In [18], for sequences of computations in Petri nets, we have given an algorithm for extracting partial orders that exhibit event structure semantics[1]. In the following, we carry these ideas to CTMCs of process algebra simulations by tracing the consumption and production effect of each event. This way, we extract the information on the flow of resources in simulations as partial orders. We then apply transformations to these partial orders for flux analysis. We illustrate these ideas first on a simple example, and then on a published model of Rho GTP-binding proteins [14, 5].

We restrict the presentation in this paper to the models that are given as sets of chemical reactions, and we use the stochastic π calculus and its implementation language SPiM [22]. However, we believe that the ideas presented in this paper are applicable for a more general class of models and to a broader spectrum of modelling languages.

2 Processes of Biology

In this section, we describe how stochastic π calculus can be used to model biological systems, e.g., as systems of chemical reactions [5] or as systems of entities with more complex structures, e.g., polymers [4]. In stochastic π calculus, the basic building blocks are processes which are defined as follows.

Definition 1 *[5] Syntax of the stochastic π calculus:* processes *range over $P, Q, \ldots$ Below $fn(P)$ denotes the set of names that are free in P.*

`P,Q::=`	`M`	*Choice*	`M::=`	`()`	*Null*
—	`X(n)`	*Instance*	—	`π; P`	*Action*
—	`P | Q`	*Parallel*	—	`do π1;P1 or...or πN;PN`	*Actions*
—	`new x P`	*Restriction*			
			`π::=`	`?x(m)*r`	*Input*
`E::=`	`{}`	*Empty*	—	`!x(n)*r`	*Output*
—	`E,X(m) = P`	*Definition,* $fn(P) \subseteq m$	—	`delay@r`	*Delay*

[1] The algorithm in [18] is presented on multiplicative exponential linear logic encodings of Petri nets.

Expressions above are considered equivalent up to the least congruence relation given by the equivalence relation $\equiv$ defined as follows.

$$
\begin{array}{lrcl}
 & \texttt{P | ()} & \equiv & \texttt{P} \\
 & \texttt{P | Q} & \equiv & \texttt{Q | P} \\
 & \texttt{P | (Q | R)} & \equiv & \texttt{(P | Q) | R} \\
\texttt{X(m) = P} & \texttt{X(n)} & \equiv & \texttt{P}\{\texttt{m:=n}\} \\
 & \texttt{new x ()} & \equiv & \texttt{()} \\
 & \texttt{new x new y P} & \equiv & \texttt{new y new x P} \\
x \notin fn(P) & \texttt{new x (P | Q)} & \equiv & \texttt{P | new x Q}
\end{array}
$$

While implementing models in the stochastic π calculus, we follow the abstraction of the biochemical species as entities that can change state. The state changes can be spontaneous or result from the interactions of the species with other species. We denote different states of the species with processes. Because the state of a species is a process with different state transition capabilities, a process `P` can choose stochastically between zero or more alternative behaviours. In the language of SPiM, we write the choice of N processes as `do P1 or ... or PN`. A choice of only one process is written as `P1`, while the empty choice is written as `()`. A parallel composition of N processes is written as `P1 | ... | PN`. A process can also be given a name `X` with parameter `m`, written `let X(m) = P`. By using these constructs, we can compose processes to construct models and incrementally extend them to build larger models when desired.

The reduction rules of the calculus are as follows.

Definition 2 *[5] Reduction in the stochastic π calculus.*

$$
\begin{array}{lll}
(1) & \texttt{do delay@r; P or ...} & \xrightarrow{r} \quad \texttt{P} \\
(2) & \texttt{(do !x(n)*r1; P1 or...) | (do ?x(m)*r2; P2 or...)} & \xrightarrow{\rho(x)\cdot r1\cdot r2} \quad \texttt{P1 | P2}\{\texttt{m:=n}\} \\
(3) & \texttt{P} \xrightarrow{r} \texttt{P'} & \texttt{new x P} \xrightarrow{r} \texttt{new x P'} \\
(4) & \texttt{P} \xrightarrow{r} \texttt{P'} & \texttt{P | Q} \xrightarrow{r} \texttt{P' | Q} \\
(5) & \texttt{Q} \equiv \texttt{P} \xrightarrow{r} \texttt{P'} \equiv \texttt{Q'} & \texttt{Q} \xrightarrow{r} \texttt{Q'}
\end{array}
$$

A species can spontaneously change state after a delay or as a result of a stochastic interaction with another species. The stochastic behaviour of the processes is delivered by the rate of the delay or interaction actions that the processes can perform: a process can perform a delay at rate r and then do `P`, written `delay@r;P`. The rate r is a real number value denoting the rate of an exponential distribution. A process can also send a value n on channel x with weight w_1 and then do P_1, written `!x(n)*w1;P1`, or it can receive a value m on channel x with weight w_2 and then do P_2, written `?x(m)*w2;P2`. With respect to the reduction semantics of SPiM, these complementary send and receive actions can synchronise on the common channel x and evolve to `P1 | P2`$\{$`m := n`$\}$, where m is replaced by n in process P_2. This allows messages to be exchanged from one process to another. Each channel name x is associated with an underlying rate given by $\rho(x)$. The resulting rate of the interaction is given by $\rho(x)$ times the weights w_1 and w_2. If no weight is given then a default weight of 1 is used. The operator `new x@r:t P` creates a fresh channel x of rate r to be used in the process P, where t is the type of the channel. When a process is prefixed with the declaration of a fresh channel, that channel remains private to the process and does not

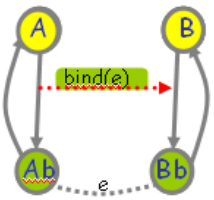


```
new bind@r1:chan(chan)
let A() = ( new e@r2:chan
!bind(e); Ab(e) )
and Ab(e:chan) = !e; A()
let B() = ( ?bind(e); Bb(e) )
and Bb(e:chan) = ?e; B()
```

```
new bind@r1:chan()
let A() = !bind; AB()
and AB() = delay@r2; ( A() | B() )
and B() = ( ?bind(); () )
```

Figure 1: Two different encodings in SPiM of a model of the association of the species A and B to form a complex, and their dissociation: on the left, we have a model and its graphical representation, where the usage of the private name `e` for the bond between the species `Ab` and `Bb` permits the monitoring of the individual species in the complex after the association. The model on the right abstracts away from this information within a simpler representation.

conflict with any other channel. By using these constructs, we can describe the dynamics of a biological system as a model in the language of SPiM.

Example 3 *Consider the biochemical species `A` and `B` which can associate with rate r_1 to form a complex and dissociate with rate r_2. In Figure 1, we depict two different encodings of this model in SPiM.*

For an in depth exposure to the syntax and semantics of the stochastic π calculus that is implemented in SPiM and examples of models with varying structures, we refer to [22, 5, 3, 1, 4, 19].

3 Causality as Partial Order

The stochastic semantics of the π calculus models in SPiM are given with continuous time Markov chains (CTMC). These CTMCs are infinite sets that collect the possible simulation trajectories of the modelled systems. In each possible trajectory of a process model, the duration of each state change is delivered by an exponential distribution from a continuous interval. Then, a simulation with a model is essentially a sequence of state transitions of the underlying model, where each transition is stamped with a time constant that imposes a total order on these transitions. In order to see this on an example, let us first define formally the class of models that we discuss in this paper.

Definition 4 (model) *Biochemical species are denoted with $A,B,P,Q,\ldots$. A model $\mathscr{M}$ is a pair $(\mathscr{I},\mathscr{R})$ where $\mathscr{I}$ is a multiset[2] of species denoting the initial state of the model and $\mathscr{R}$ is a finite set of chemical reactions of the form*

$$\mathsf{r} : A \to_\rho P_1 + \ldots + P_k \qquad or \qquad \mathsf{r} : A + B \to_\rho P_1 + \ldots + P_k$$

such that $k \in \mathbb{N}$, r is the name of the rule, and $\rho \in \mathbb{R}^+$ is the rate of the reaction.

Example 5 *Consider the model with the reactions below and the initial state $\mathscr{I} = \{\!|A|\!\}$, which can be implemented in SPiM as depicted in Figure 2. On the left-hand-side in Figure 3, we have a simulation output with this model.*

$$\mathsf{r}_1 : A \to_{1.0} P + P \qquad \mathsf{r}_2 : P \to_{1.0} B \qquad \mathsf{r}_3 : P \to_{1.0} C \qquad \mathsf{r}_4 : B + C \to_{1.0} D$$

[2]Multisets are denoted by the curly brackets "$\{\!|$ $|\!\}$". $\dot\cup$, $\dot-$ and $\dot\subseteq$ denote the multiset operations corresponding to the usual set operations $\cup$, $-$ and $\subseteq$, respectively.

```
directive sample 1000.0           new ch@r4:chan()                    and B() = ?ch; D()
directive plot A(); P();                                              and C() = !ch; ()
               B(); C(); D()      let A() = delay@r1; (P() | P())
                                                                      and D() = ()
val r1 = 1.0    val r2 = 1.0      and P() = do delay@r2; B()
val r3 = 1.0    val r4 = 1.0                or delay@r3; C()          run 1 of A()
```

Figure 2: A SPiM implementation of the model given in Example 5.

A simulation on such a process model can be seen as the interleavings of the computations of a place/transition Petri net, which can be infinite, e.g., in the case of polymerisation models [4, 7]: in Petri nets, each transition has incoming arrows from places, containing tokens that are consumed as a result of the transition, and it has outgoing arrows to places, containing the tokens that are produced as a result of the transition. Then, each '`delay`' action is a transition with a single incoming place, and each action resulting from the interaction of input ('`?`') and output ('`!`') actions is a transition with two incoming places for the input and output actions. For the purpose of this paper, we restrict the models to those, which can be expressed as finite sets of chemical reactions. This restriction allows us to denote each model interchangeably as a finite set of chemical reactions as well as the corresponding Petri net or the (equivalence class of the) SPiM implementation (since there does not exist a unique implementation for each set of reactions in SPiM).

Example 6 *Consider the Petri net depicted in Figure 4, which is the net underlying the model given in Example 5 and implemented in Figure 2.*

The consideration of a simulation trajectory of a process model from the point of view of Petri nets remains in agreement also with the CTMC semantics that imposes a total order on the transitions (see, e.g., [20]). However, when these transitions are inspected from the point of view of their dependencies on one another with respect to their production/consumption relationships, it is possible to relax this total order into a partial order by abstracting away from the time stamps of the state transitions.

Example 7 *Consider the model given in Example 5. In a simulation on this model, the reactions* r_2 *and* r_3 *are totally ordered due to the time stamps on them. However, we can relax this total order into a partial order with respect to the production/consumption relationship between the transitions as depicted in Figure 3.*

In fact, the underlying Petri net of a process model hints this partial order structure on the transitions, as it can be seen on the example net depicted in Figure 4. However, the possible conflicts in simulations between various transitions with respect to the availability of resources remain implicit in the structure of a net. For example, consider a simulation state with the Petri net in Figure 4, where there is a token in place `P`, and thus there is a conflict between the transitions r_2 and r_3. Although this conflict can be observed by inspecting multiple outgoing arrows from places, it is not always explicit in the structure of more complex Petri nets.

Partial orders reflecting dependencies in computations have been studied as non-interleaving models of concurrency: in this setting, the synchronisation of concurrent transitions is realized by their common successors and predecessors, which is in agreement with the notion of state transitions in Petri nets. When there are no resource conflicts between two partially ordered threads, they can take place in parallel (but not necessarily simultaneously), and their common predecessors and successors provide

a synchronisation mechanism. This is because the common predecessors deliver the resources for the parallel threads, and the completion of the execution of the threads delivers the resources required by their common successors. This view also provides a model of causal flow in the execution.

A certain model of concurrency, which is closely related to Petri nets [21], namely *event structures*, captures these ideas: in an event structure, each instance of a state transition is an event. The dependencies of events of a concurrent system are given with a partial order, and non-determinism is captured by a conflict relation, which is a symmetric irreflexive relation of events. When two events are in conflict, the execution of one of them instead of the other determines a different state space ahead.

Definition 8 (labelled event structures) *A labelled event structure (LES) is a structure* $(E, \leq, \#, \mathscr{L}, \ell)$, *where*

(i.) E *is a set of events;*

(ii.) $\leq \subseteq E^2$ *is a partial order such that for every* $\mathsf{e} \in E$ *the set* $\{\mathsf{e}' \in E \,|\, \mathsf{e}' \leq \mathsf{e}\}$ *is finite;*

(iii.) the conflict relation $\# \subseteq E^2$ *is a symmetric and irreflexive relation such that if* $\mathsf{e}\#\mathsf{e}'$ *and* $\mathsf{e}' \leq \mathsf{e}''$ *then* $\mathsf{e}\#\mathsf{e}''$ *for every* $\mathsf{e}, \mathsf{e}', \mathsf{e}'' \in E$;

(iv.) $\mathscr{L}$ *is a set of labels;*

(v.) $\ell : E \to \mathscr{L}$ *is a labelling function.*

There are standard techniques in the literature for obtaining a labelled event structure from transition systems and from other models of concurrency [27]. In particular, in [18] we present an application of these techniques for obtaining a labelled event structure from the multiplicative exponential linear logic encodings of Petri nets. We can analogously carry these ideas to the setting of the process models: for every model $\mathscr{M}$, we use the operational semantics of the stochastic π calculus, given with the reduction rules in Definition 2, as a transition system. This way, we apply the techniques presented in [18] to obtain the $\mathsf{LES}[\![\mathscr{M}]\!]$ for the model $\mathscr{M}$.

Example 9 *We obtain the event structure depicted in Figure 4 for the model in Example 5.*

Definition 10 *Given a LES* $(E, \leq, \#, \mathscr{L}, \ell)$, *for any event* $\mathsf{e} \in E$, $\lfloor \mathsf{e} \rfloor$ *denotes the set* $\{\mathsf{e}' \in E | \mathsf{e}' < \mathsf{e}\}$ *of* causes *of event* e. *We say that* $\mathscr{C} \subseteq E$ *is a* configuration *if and only if (i.) for all* $\mathsf{e} \in \mathscr{C}$ *we have that* $\lfloor \mathsf{e} \rfloor \subset \mathscr{C}$; *(ii.) for all* $\mathsf{e}, \mathsf{e}' \in \mathscr{C}$, *it is not the case that* $\mathsf{e}\#\mathsf{e}'$.

Example 11 *Consider the event structure given in Figure 4. The sets* $\{\mathsf{e}_1, \mathsf{e}_2, \mathsf{e}_3, \mathsf{e}_4\}$ *and* $\{\mathsf{e}_1, \mathsf{e}_2, \mathsf{e}_2'\}$ *are configurations.*

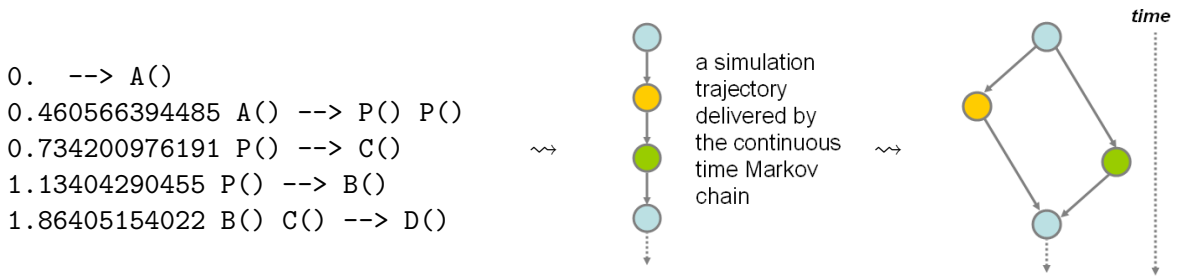

Figure 3: Graphical representation of the extraction of a partial order that reflects the production/consumption relationship of the transitions in a simulation with the model in Example 7.

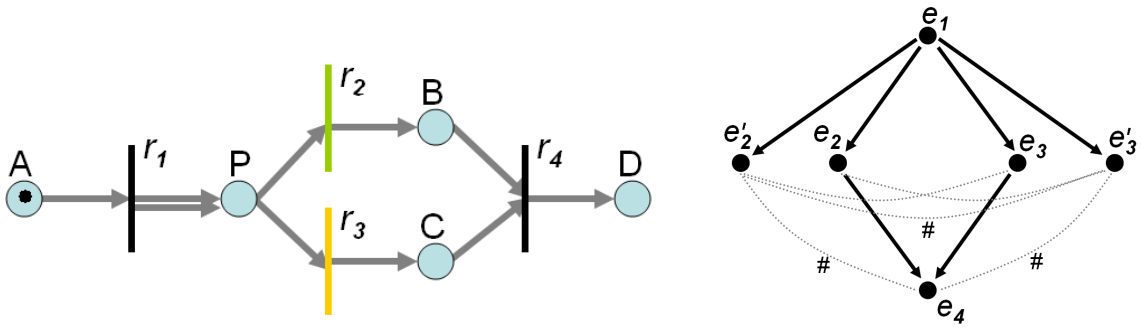

Figure 4: The Petri net of the model given in Example 5 and the LES of this model, where the subscripts of the events correspond to the subscripts of the reactions(transitions) that they refer to. The dashed lines denote the conflict relation #.

In [18], we have given an algorithm for extracting configurations from transition histories of Petri nets. Below, we analogously carry these ideas to the setting of the process models being discussed here: the CTMCs in SPiM treat the processes as resources in the sense that processes representing species are consumed and new ones are produced as a result of a reduction with SPiM. 'Resource consciousness' is the crucial ingredient that delivers the LES semantics in [18]. We can thus extract a partial order that delivers the causal dependencies of the transitions of a particular simulation as sketched in Figure 3. Let us first collect some definitions that we need to formally describe this procedure on SPiM simulations.

Definition 12 (simulation state) *Let $\mathscr{M} = (\mathscr{I}, \mathscr{T})$ be a model with the reactions $\mathsf{r}_1, \ldots, \mathsf{r}_n$. A* simulation state *of $\mathscr{M}$, denoted with $\mathscr{Z}$, is a multiset of species such that each species in $\mathscr{Z}$ is parameterised with a label $\mathsf{k} \in \mathbb{N}^+$ denoting an id, a label $p, q \in \{\mathsf{init}, \mathsf{r}_1, \ldots, \mathsf{r}_n\}$ denoting the reaction that created this species, and $t \in \mathbb{R}^+$ denoting its creation time. The* initial simulation state *$\mathscr{Z}_0$ for the initial state $\mathscr{I}$ of a model is obtained from $\mathscr{I}$ by assigning a* unique *label $\mathsf{k} \in \mathbb{N}^+$ to each species and marking each species with* init *and the time* 0*.*

In SPiM, we can implement the notion of a simulation state by decorating each process with an integer valued `id`, which is communicated during the reduction of the process to its continuation.

Example 13 *Consider the SPiM program given in Figure 5, which is obtained from the program in Figure 2 by assigning an* `id` *to each process. Here, we have initially four instances of the process A. Thus, $\mathscr{Z}_0 = \{\!|A(1,\mathsf{init},0), A(2,\mathsf{init},0), A(3,\mathsf{init},0), A(4,\mathsf{init},0)|\!\}$ is the initial simulation state for the initial state of the model implemented in Figure 5.*

Definition 14 (simulation trajectory) *Let $\mathscr{M} = (\mathscr{I}, \mathscr{T})$ be a model. A* simulation trajectory *$\mathscr{S}$ on $\mathscr{M}$ is a list of structures of the form $(\mathsf{t}, \mathsf{L}, \mathsf{R})$, called* transition instances*, where $\mathsf{t} \in \mathbb{R}^+$ is the time stamp of the transition. L and R are multisets of species that we call* consumed *and* produced *species, respectively. We assume that for each pair (L, R) there is a reaction r in $\mathscr{T}$ and the species on the left-hand-side and right-hand-side of r, respectively, are exactly those in L and R. In this case, we say that* $(\mathsf{t}, \mathsf{L}, \mathsf{R})$ is an instance of r. *We use $[]$ to denote the empty trajectory and the operator '$\bullet$' to denote the concatination of a transition with a simulation trajectory, e.g., $\mathscr{S} = (\mathsf{t}, \mathsf{L}, \mathsf{R}) \bullet \mathscr{S}'$.*

We use the simulation trajectories for representing the outcome of simulations with SPiM models.

```
directive sample 1000.0          let A(id:int) = delay@r1;              and C(id:int) = !ch; ()
directive plot A(); P();                           (P(id) | P(id))
              B(); C(); D()                                            and D(id:int) = ()
                                 and P(id:int) = do delay@r2; B(id)
val r1 = 1.0    val r2 = 1.0                     or delay@r3; C(id)     run ( A(1) | A(2) |
val r3 = 1.0    val r4 = 1.0                                                 A(3) | A(4) )
                                 and B(id:int) = ?ch; D(id)
new ch@r4:chan()
```

Figure 5: A SPiM implementation of the model given in Example 5 where each process is assigned an id as a parameter that is communicated during reductions.

```
0.  --> A(4) A(3) A(2) A(1)                  1.53959162309 P(2)  --> B(2)
0.362742117504 A(4)  --> P(4) P(4)           1.61357605349 P(3)  --> B(3)
0.403041278461 P(4)  --> B(4)                1.62828014739 P(1)  --> B(1)
0.533386757223 P(4)  --> C(4)                1.74376163407 P(2)  --> C(2)
1.38225471287 A(1)  --> P(1) P(1)            1.93175167917 P(1)  --> C(1)
1.45347041154 A(2)  --> P(2) P(2)            2.09975124488 B(4) C(1)  --> D(4)
1.51272758278 A(3)  --> P(3) P(3)            2.10580589848 B(3) C(4)  --> D(3)
1.52969767363 P(3)  --> B(3)                 2.14571167381 B(2) C(2)  --> D(2)
```

Figure 6: A SPiM output of a simulation with the model given with the code in Figure 5.

Example 15 *Consider the simulation output given in Figure 6. We denote this output as the simulation trajectory $\mathscr{S}$, where $\mathscr{S}'$ is a simulation trajectory that contains the transitions after the time point* 1.0*.*

$$\mathscr{S} = \quad (0.362, \{\!|A(4)|\!\}, \{\!|P(4),P(4)|\!\}) \bullet (0.403, \{\!|P(4)|\!\}, \{\!|B(4)|\!\}) \bullet (0.533, \{\!|P(4)|\!\}, \{\!|C(4)|\!\}) \bullet \mathscr{S}'$$

Definition 16 (simulation configuration) *Let $\mathscr{M} = (\mathscr{I}, \mathscr{T})$ be a model with the reactions $\mathsf{r}_1, \ldots, \mathsf{r}_k$. The* simulation configuration *for a simulation trajectory $\mathscr{S}$ and an initial simulation state $\mathscr{Z}_0$, denoted by $\mathsf{C}_{\mathscr{S},\mathscr{Z}_0}$, is the structure $\mu(\mathscr{S}, \mathscr{Z}_0)$, where the recursive function μ on the pairs of simulation trajectories and simulation states is defined as follows.*

- *if $\mathscr{S} = (\mathsf{t}, \mathsf{L}, \mathsf{R}) \bullet \mathscr{S}'$ such that $\mathsf{L} = \{\!|A(m)|\!\}$, $\mathsf{R} = \{\!|P_1(m), \ldots, P_k(m)|\!\}$,*
  - *there is a reaction $\mathsf{r} \in \{\mathsf{r}_1, \ldots, \mathsf{r}_k\}$ such that $(\mathsf{t}, \mathsf{L}, \mathsf{R})$ is an instance of r, and*
  - *for transition label p and time label t', $A(m,p,t') \in \mathscr{Z}$,*

    then $\mu(\mathscr{S}, \mathscr{Z}) = \{\langle (m,\ p, t'), (m, \mathsf{r}, \mathsf{t}) \rangle\}$
    $\cup\ \mu(\mathscr{S}', (\mathscr{Z} \dot{-} \{\!|A(m,p,t')|\!\}) \dot{\cup} \{\!|P_1(m,\mathsf{r},\mathsf{t}), \ldots, P_k(m,\mathsf{r},\mathsf{t})|\!\})$.
- *if $\mathscr{S} = (\mathsf{t}, \mathsf{L}, \mathsf{R}) \bullet \mathscr{S}'$ such that $\mathsf{L} = \{\!|A(m_1), B(m_2)|\!\}$, $\mathsf{R} = \{\!|P_1(x), \ldots, P_k(x)|\!\}$, $x = m_1 \vee x = m_2$,*
  - *there is a reaction $\mathsf{r} \in \{\mathsf{r}_1, \ldots, \mathsf{r}_k\}$ such that $(\mathsf{t}, \mathsf{L}, \mathsf{R})$ is an instance of r, and*
  - *for transition labels p, q and time labels t', t'', $A(m_1, p, t') \in \mathscr{Z}$ and $A(m_2, q, t'') \in \mathscr{Z}$,*

  then $\mu(\mathscr{S}, \mathscr{Z}) = \{\langle (m_1, p, t'), (x, \mathsf{r}, \mathsf{t}) \rangle, \langle (m_2, q, t''), (x, \mathsf{r}, \mathsf{t}) \rangle\}$
  $\cup\ \mu(\mathscr{S}', (\mathscr{Z} \dot{-} \{\!|A(m_1,p,t'), A(m_2,q,t'')|\!\}) \dot{\cup} \{\!|P_1(x,\mathsf{r},\mathsf{t}), \ldots, P_k(x,\mathsf{r},\mathsf{t})|\!\})$.
- *Otherwise $\mu(\mathscr{S}, \mathscr{Z}) = \emptyset$.*

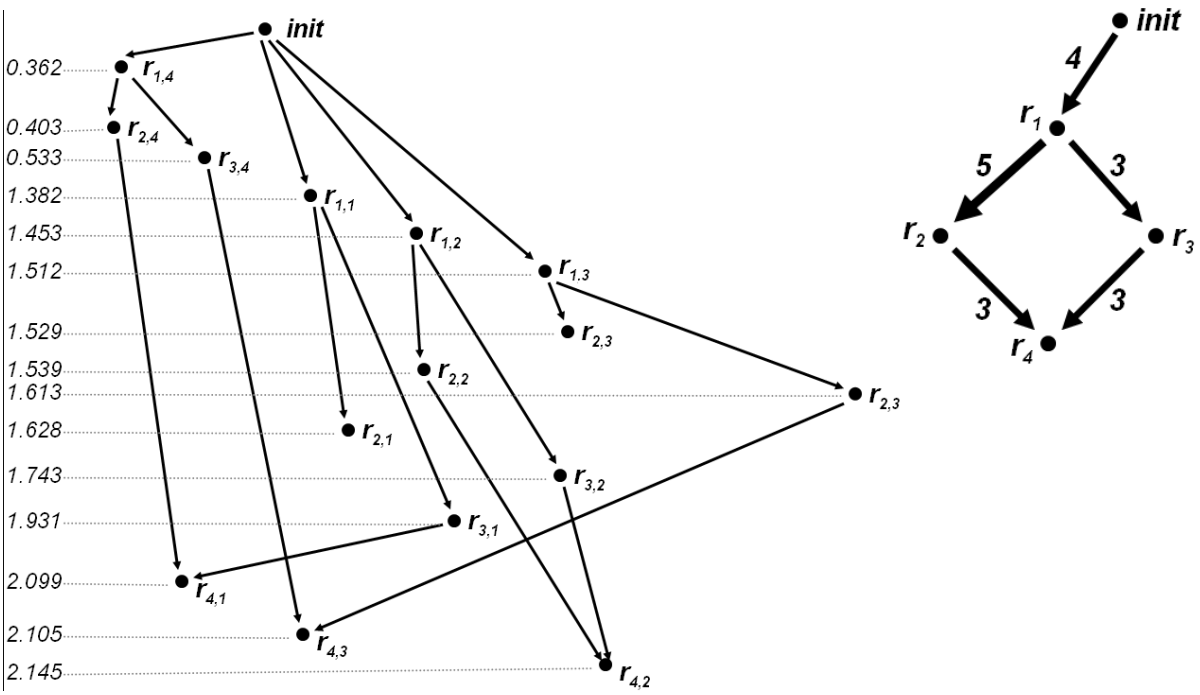

Figure 7: The simulation configuration obtained from the simulation trajectory delivered by the simulation output in Figure 6, and the graphical representation of the flux configuration obtained from it by merging the events that are instances of the same reactions. On the left, each node (x, r_i, t) is abbreviated with $\mathsf{r}_{i,x}$. On the right, the thickness of the arrows are proportional with the weights of the edges.

Example 17 *Consider the model $\mathscr{M}$ with the SPiM code in Figure 5, the initial simulation state $\mathscr{Z}_0$ given in Example 13 and the simulation trajectory $\mathscr{S}$ given in Example 15. We get the simulation configuration $\mathsf{C}_{\mathscr{S},\mathscr{Z}_0}$ depicted in Figure 7.*

The following proposition is a special case of a more general discussion presented in [18].

Proposition 18 *Let $\mathscr{M}$ be a model with an initial simulation state $\mathscr{Z}_0$ and a simulation trajectory $\mathscr{S}$. The transitive reflexive closure of the simulation configuration $\mathsf{C}_{\mathscr{S},\mathscr{Z}_0}$ is a configuration in $\mathsf{LES}[\![\mathscr{M}]\!]$.*

4 Quantitative Flux Analysis on Models

A simulation configuration contains the information on the causal dependencies of the transitions of a simulation. These causal dependencies are expressed as a partial order of individual events. However, despite the partial order representation of the causal flow, it remains possible to read the total order of the transitions given in the simulation with respect to the time stamps of these events.

In this respect, a simulation configuration is a representation of a simulation, where the previously implicit information is made explicit. Although such a representation is rich in information, it is difficult to make observations about the quantitative behaviour of the modelled system. Thus, a simulation configuration can be seen as raw data that needs to be processed further for analysis.

The idea here is to apply various transformations to the partially ordered structures of simulation configurations to extract useful information on the dynamics of the system. There are a variety of possible choices for such transformations. In the following, we consider a transformation, which can provide a means for *quantitative flux analysis* in the stochastic setting of process algebra models. In this transformation, we merge the events that are instances of the same reaction to the same node, while counting the number of edges that collapse to a single edge. This way, we assign weights to the edges of the graph and obtain a cyclic graph with weights.

Definition 19 (flux configuration) *Let $\mathsf{C}_{\mathscr{S},\mathscr{Z}_0}$ be a simulation configuration. The flux configuration of $\mathsf{C}_{\mathscr{S},\mathscr{Z}_0}$, denoted by $\mathsf{F}_{\mathscr{S},\mathscr{Z}_0}$, is the set that contains the triples of the form (p,q,n) such that $(p,q,n) \in \mathsf{F}_{\mathscr{S},\mathscr{Z}_0}$ if and only if there are n number of pairs $\langle (i,p,t),(j,q,t')\rangle \in \mathsf{C}_{\mathscr{S},\mathscr{Z}_0}$ for all the possible i,j,t,t'.*

Example 20 *Consider the simulation configuration $\mathsf{C}_{\mathscr{S},\mathscr{Z}_0}$ depicted on the left-hand-side in Figure 7. We obtain the flux configuration $\mathsf{F}_{\mathscr{S},\mathscr{Z}_0} = \{(\mathsf{init},\mathsf{r}_1,4),(\mathsf{r}_1,\mathsf{r}_2,5),(\mathsf{r}_1,\mathsf{r}_3,3),(\mathsf{r}_2,\mathsf{r}_4,3),(\mathsf{r}_3,\mathsf{r}_4,3)\}$ which is depicted as the graph on the right-hand-side in Figure 7, where the numbers on the edges are the weights of the edges.*

In comparison to the simulation trajectories and the simulation configurations, the flux configurations provide a more intelligible representation of the causal flow in a simulation from a quantitative point of view. In particular, in a flux configuration, the quantitative information on the flux of the species between reactions in the system is highlighted with respect to the simulation. This way it becomes possible to make observations on the system that are impossible, for example, by counting the number of species or reactions. However, it is important to note that there can be various choices to be made while processing a simulation configuration. For example, when we consider the transformation proposed above, we could have considered only causally independent events while merging them. While this criteria would not alter the graph in Figure 7, it would deliver different graphs for the model that we discuss in the next section.

5 A Biological Model: Rho GTP-binding Proteins

In this section, we apply the ideas discussed above to a model of a biological system, that is, *Rho GTP-binding proteins* [17, 14, 5].

The Rho GTP-binding proteins constitute a distinct family within the super-family of Ras-related small GTPases with twenty-two identified mammalian members, including Rho, Rac and Cdc42 [11]. Rho GTP-binding proteins serve as molecular switches in various subcellular activities, regulating a variety of cell functions, including actin organisation and cell shape, cell adhesion, cell motility, membrane trafficking and gene expression [2]. Their role can be perceived as regulating the transmission of an incoming signal further to effectors in a molecular module by cycling between inactive and active states, depending on being GDP or GTP bound, respectively. As depicted in Figure 8, GDP/GTP cycling is regulated by guanine nucleotide exchange factors (GEFs) that promote the GDP dissociation and GTP binding, whereas GTPase-activating proteins (GAPs) have the opposite effect and stimulate the hydrolysis of Rho-GTP into Rho-GDP. In the active GTP-bound state, Rho proteins interact with and activate downstream effectors.

In [14], Goryachev and Pokhilko give an ordinary differential equations (ODE) model of the Rho GTP-binding proteins. The structure of this ODE model is depicted on the right-hand-side in Figure 8: the three forms of the Rho protein (GDP-bound RD, GTP-bound RT, and nucleotide free R) in the middle layer form complexes with GEF (E) in the bottom layer and with GAP (A) in the top layer. All

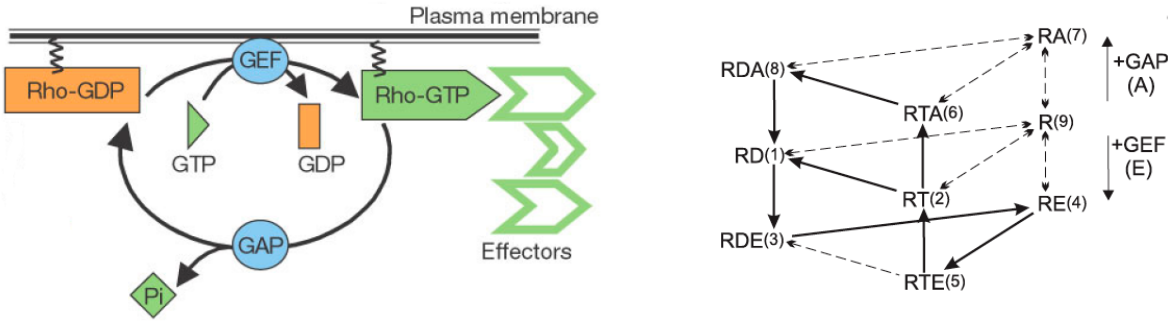

Figure 8: Left: Rho GTP-binding protein cycle, adapted with permission from Macmillan Publishers Ltd: *Nature* [11], copyright 2002. Right: the structure of the Rho GTP-binding proteins model given in [14]. In the graph, R denotes the Rho GTP-binding protein, whereas RD and RT denote its GDP and GTP bound forms respectively. A and E denote GAP and GEF, respectively. Thus, RDE, for example, denotes the protein complex formed by RD and E.

the reactions except GTP hydrolysis ($2 \to 1$, $6 \to 8$, $5 \to 3$) are reversible. In their model, Goryachev and Pokhilko use the quantitative biochemical data on the Cdc42p member of the Rho family proteins. This results in an explanation of the experimentally observed rapid cycling of the Rho GTP-binding proteins between their GDP-bound off states and GTP-bound on states while displaying high activity, measured by the relative concentration of the GTP-bound Rho proteins (RT in Figure 8). The authors argue that GEF and GAP play distinct and separable roles in cycling control: the activity of Rho proteins is mainly delivered by the activity of the GEF and the turnover rate is a function of the GAP concentration. Therefore, to achieve a high activity and turnover rate simultaneously, the concentrations of GEF and GAP should be tightly controlled. Moreover, at large E_0 and A_0, only a subset of the fluxes [3] of the original model is significant, while the remaining fluxes have negligible values. To test this hypothesis, Goryachev and Pokhilko introduce a reduced model and provide a comparison with the original model with respect to the flux vectors that substantiates the claim. Goryachev and Pokhilko argue that in the efficient regime the operation of the GEF-GAP control module is based on two linear pathways: the GEF arm $1 \to 3 \to 4 \to 5 \to 2 \to 1$ and the GAP arm $2 \to 6 \to 8 \to 1$, which are indicated by solid arrows in Figure 8.

In [5], Cardelli et al give a stochastic π calculus model of the Rho GTP-binding proteins, which is based on the ordinary differential equations model of [14]. The model in [5], displays an excellent agreement with the ODE model of [14] with respect to the RT activity on simulations with varying model structures and different regimes of initial concentrations. In the following, we consider this model for flux analysis by employing our software tool that implements the ideas above.

[3] In [14], the flux J_{lm} for a reaction that connects species l and m is defined with respect to the species concentrations and the rate constants, e.g., flux J_{13} connecting RD and RDE is $J_{13} = k_{13}.\mathsf{RD}.\mathsf{E} - k_{31}.\mathsf{RDE}$ where k_{13} and k_{31} are the corresponding reaction rates.

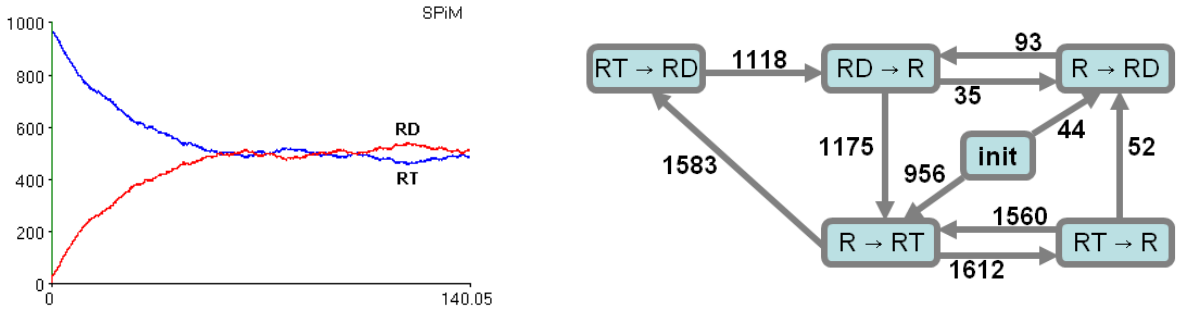

Figure 9: A simulation with the reduced model, given with the mid layer of the model depicted in Figure 8, and the graph representation of the flux configuration of a simulation for the interval $0 < t < 140$.

5.1 Rho without Regulators

At a first step for flux analysis with respect to simulations on a stochastic π calculus model of the Rho GTP-binding proteins, we consider the mid-layer of the model depicted on the right-hand-side of Figure 8. The SPiM code of the complete model is given in Appendix A. For the simulations on the reduced model, we run simulations on the complete model where the initial number of species for A and E are set as 0. The initial number of R is set as 1000. Because a variation on R levels does not cause a significant variation in the simulation behaviour as it can be observed from the results in [14] and [5], here we do not consider variations on the R_0. The plot that displays the evolution of the number of species at a simulation that is run until the time $t = 140$ min. is depicted [4] on the left-hand-side of Figure 9.

The graph representation of the flux configuration for the time interval $0 < t < 140$ of a simulation is given on the right-hand-side of the Figure 9. In this plot, we observe that after the start of the simulation, the reactions $R \to RD$ and $R \to RT$ are competing for R and the flux ratio of these reactions reflect the bias of the rate constants of these reactions towards the reaction $R \to RT$. Because the flux configuration is for the simulation until the time $t = 140$, the flux of the resources demonstrates the system's accumulation of steady state numbers of species from the start of the simulation: the initial concentrations are $R_0 = 1000$, $RD_0 = 0$ and $RT_0 = 0$. At the end of the simulation we have $R = 1$, $RD = 503$ and $RT = 496$. When we examine each reaction in the graph with respect to the weights of their incoming and outgoing arrows, we observe that the quantities correspond to those accumulated at the end of the simulation as demonstrated

[4] The time unit of the model in [14] is given in minutes.

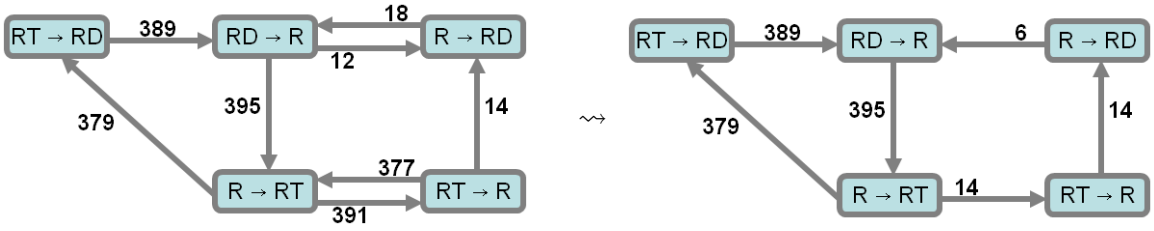

Figure 10: Graph representation of the flux configuration of the simulation for the interval $100 < t < 140$.

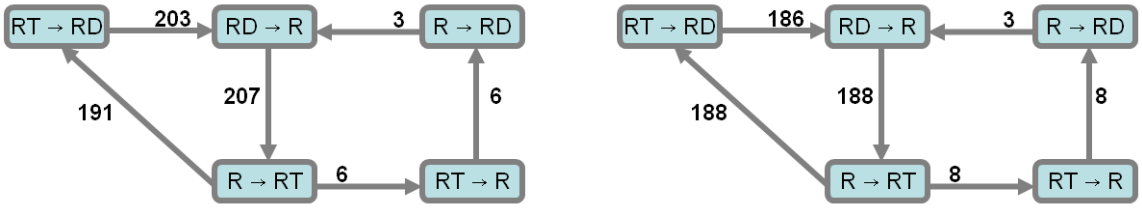

Figure 11: Graph representations of the flux configurations of the simulations for the intervals $100 < t < 120$ and $120 < t < 140$.

below and they sum up to 1000.

$$\left.\begin{array}{l}\mathsf{RT} \to \mathsf{RD} : 1583 - 1118 = 465\,\mathsf{RD} \\ \mathsf{R} \to \mathsf{RD} : (35+44+52) - 93 = 38\,\mathsf{RD}\end{array}\right\} 503\mathsf{RD} \qquad \left.\begin{array}{l}\mathsf{RD} \to \mathsf{R} : (1118+93) - (35+1175) = 1\,\mathsf{R} \\ \mathsf{RT} \to \mathsf{R} : 1612 - (1560+52) = 0\,\mathsf{R}\end{array}\right\} 1\mathsf{R}$$

$$\mathsf{R} \to \mathsf{RT} : (1560+956+1175) - (1583+1612) = 496\,\mathsf{RT}$$

By relying on the data that the cycling period of the system is 100 min [14], we analyse the flux configuration on the same simulation for the time interval $100 < t < 140$. This provides an examination of the steady-state behaviour of the system. The graphical representation of the flux configuration for this interval is given on the left-hand-side of Figure 10. On the right-hand-side of this Figure, we simplify this graph by taking the sum of the fluxes for the cases, where there are opposite directional fluxes between two reactions. For example, we reduce the two arrows between the reactions $\mathsf{R} \to \mathsf{RT}$ and $\mathsf{RT} \to \mathsf{R}$ to a single arrow. Below we examine the incoming and outgoing fluxes for each reaction.

$$\begin{array}{lll}\mathsf{RT} \to \mathsf{RD} : 379 - 389 = -10\,\mathsf{RD} & \mathsf{RD} \to \mathsf{R} : 395 - (389+6) = 0\,\mathsf{R} & \mathsf{R} \to \mathsf{RT} : 395 - (379+14) = 2\,\mathsf{RT} \\ \mathsf{R} \to \mathsf{RD} : 14 - 6 = 8\,\mathsf{RD} & \mathsf{RT} \to \mathsf{R} : 14 - 14 = 0\,\mathsf{R} & \end{array}$$

The observation that the fluxes of the individual reactions do not add up to 0 reflects the fluctuations in the stochastic simulation. However, it is important to observe the sum $-10+8+0+0+2=0$ due to the fact that the simulation is performed on a closed system. In Figure 11, we examine the flux configuration of the interval $100 < t < 140$ further by separating it into two intervals $100 < t < 120$ and $120 < t < 140$. We observe that in these smaller intervals, the fluxes of the reactions are closer to 0.

5.2 Rho with GEF and GAP

The behaviour of the model with the regulators GEF (E) and GAP (A) in [14] is insensitive to the R levels in terms of activity given by the RT/R_0 ratio at the steady states of the simulations. The model has an activity maximum with the initial concentrations $\mathsf{R} = 1.0mM$, $\mathsf{E} = 0.776mM$ and $\mathsf{A} = 0.66\mu M$.

In order to analyse the flux of the system at the high activity regime, we run simulations with $\mathsf{R}_0 = 1000$, $\mathsf{E}_0 = 776$ and $\mathsf{A}_0 = 1$, where we take the closest positive integer number value for A_0 so that factoring of the other simulation parameters would not be required. This results in a near-maximum activity of approx 0.8 at the steady state with fluctuations due to stochastic simulation. A simulation plot with the model in Appendix A with these parameters is given on the left-hand-side of Figure 12.

We analyse the steady state behaviour of the system with respect to the simulation at this regime. The output of our tool, which displays the flux configuration of the simulation for the time interval

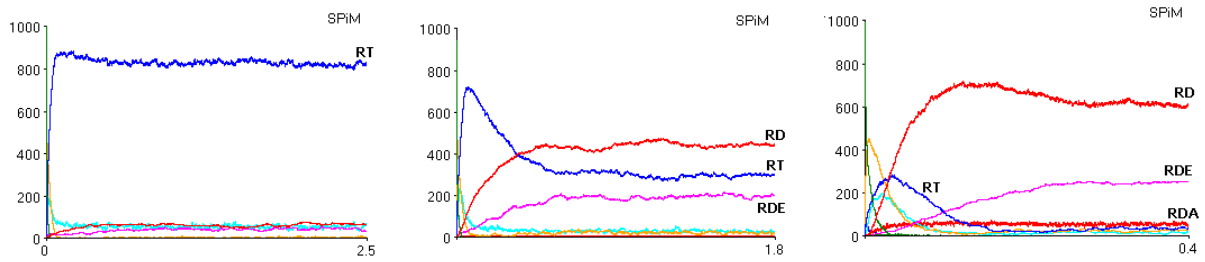

Figure 12: Simulation plots with the complete model where the initial numbers of the species are $\mathsf{R}_0 = 1000$ and $\mathsf{E}_0 = 776$. From left to right, the A_0 value is set as 1, 10 and 100. An increase in A_0 in the simulations causes decrease in the RT activity while reducing the recovery time.

$2.0 < t < 2.5$, is given in Appendix B. From this flux configuration, we obtain the top-most graph in Figure 13, where we omit the fluxes which are less than 10% of the mean of the fluxes. This delivers the more dominant flux pathway in the system at steady state, given with $2 \to 6 \to 8 \to 1 \to 3 \to 4 \to 5 \to 2$, which is in agreement with the results of [14] with the exception that the path $2 \to 1$ is not included in our graph. The presence of this flux in the pathway could be explained only with the presence of a flux from the reaction $\mathsf{RTE} \to \mathsf{RT}$ to the reaction $\mathsf{RT} \to \mathsf{RD}$. Although this flux can be read with a weight of 9 in our flux configuration ("`22 ==> 9 appears 9 times.`" in Appendix B), it is much smaller in weight in comparison to other fluxes that are depicted in the top-most graph in Figure 13. Moreover, we observe that the reaction $\mathsf{RTE} \to \mathsf{RT} + \mathsf{E}$ and its reverse reaction $\mathsf{RT} + \mathsf{E} \to \mathsf{RTE}$ deliver a strong cyclic flux, which cancels itself, thus they are not included in the graph in Figure 13.

When we carry this analysis to the simulations where A_0 is increased to 10 and 100, we get the simulation plots depicted in the middle and right-hand-side of Figure 12. We observe the same flux pathway patterns for these simulations as depicted as the middle and bottom graphs in Figure 13. However, we observe that an increase in A_0 does not only decrease the RT activity, but also increases the turnover rate.

It is important to observe that the graphs depicted in Figure 13 are generated from the model, and they reflect the predictions of the results in [14]. Along these lines, Goryachev and Pokhilko argue that a subset of the fluxes of the original model is significant in the actual biological system, while the remaining fluxes have negligible values. Goryachev and Pokhilko substantiate this prediction by comparing the reduced model with the original model. In this respect, the graphs given in Figure 13 depict a reduced model and agree with the predictions of [14] (with the exception of $2 \to 1$ as explained above). However, the graphs in Figure 13 result from the application of the ideas presented in Section 3 and Section 4 to the simulations, thus they are generated automatically, and their delivery does not require an analysis of the model or the biological system being modelled.

6 Discussion

We have shown that the event structures view of simulations discussed above provide the means for flux analysis for process algebra models in a biologically meaningful manner. However, the ideas presented here should provide a starting point for further exploration rather than being conclusive.

The relationship between process models and causality has been studied by various authors. In this regard, these previous investigations should provide touchstones for further investigations. Some of the

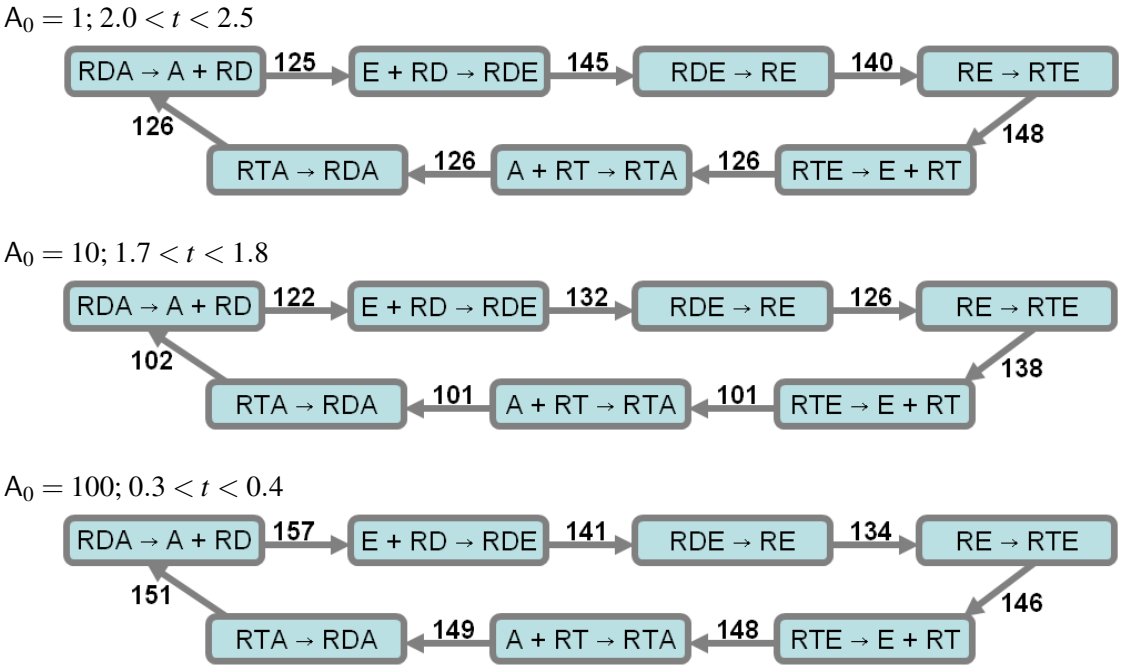

Figure 13: The graphs displaying the dominant fluxes with respect to the flux configurations obtained from simulations with $R_0 = 1000$, $E_0 = 776$ and varying initial A_0 numbers. An increase in A_0 increases the turnover rate, observed by comparing the ratio of the fluxes and the length of the time interval.

works along these lines, which also provide further reference pointers, are as follows. In [9], Danos et al draw connections between computational models of biological systems, event structures and their causality interpretation, while exploiting conflict as a mechanism of inhibition in a signalling pathway. The work by Fages and Soliman [12] attacks a similar problem by providing a formal interpretation of the relationship between reaction graphs and activation/inhibition graphs used by biologists. In [8], Curti et al apply the ideas presented in [10] to the π calculus models of biological systems where the causality information on the modelled system is retrieved by labelling the syntax tree of the process expressions.

Topics of future work include the application of the ideas above to BlenX [23] language as well as an exploration of the relationship with the syntactical approach to causality with respect to enhanced operational semantics [10].

Acknowledgements We thank Luca Cardelli for discussions and helpful suggestions, and Andrew Philips for his assistance with the SPiM language. We thank anonymous referees for valuable comments.

References

[1] R. Blossey, L. Cardelli, and A. Phillips. Compositionality, stochasticity and cooperativity in dynamic models of gene regulation. *HFSP Journal*, 2(1):17–28, 2008.

[2] X. R. Bustelo, V. Sauzeau, and I. M. Berenjeno. GTP-binding proteins of the Rho/Rac family: regulation, effectors and function in vivo. *BioEssays*, 29:356–370, 2007.

[3] L. Cardelli. Artificial biochemistry. In *Algorithmic Bioproceses*, LNCS. Springer, 2008.

[4] L. Cardelli, E. Caron, P. Gardner, O. Kahramanoğulları, and A. Phillips. A process model of actin polymerisation. In *FBTC'08*, volume 229 of *ENTCS*, pages 127–144. Elsevier, 2008.

[5] L. Cardelli, E. Caron, P. Gardner, O. Kahramanoğulları, and A. Phillips. A process model of Rho GTP-binding proteins. *Theoretical Computer Science*, 410/33-34:3166–3185, 2009.

[6] L. Cardelli and G. Zavattaro. On the computational power of biochemistry. In *AB'08*, volume 5147 of *LNCS*, pages 65–80. Springer, 2008.

[7] L. Cardelli and G. Zavattaro. Termination problems in chemical kinetics. In *CONCUR'08*, volume 5201 of *LNCS*, pages 477–491. Springer, 2008.

[8] M. Curti, P. Degano, C. Priami, and C.T.Baldari. Modelling biochemical pathways through enhanced π-calculus. *Theoretical Computer Science*, 325:111–140, 2004.

[9] V. Danos, J. Feret, W. Fontana, R. Harmer, and J. Krivine. Rule-based modelling of cellular signalling. In *CONCUR'07*, volume 4703 of *LNCS*, pages 17–41. Springer, 2007.

[10] P. Degano and C. Priami. Enhanced operational semantics: A tool for describing and analyzing concurrent systems. *ACM Computing Surveys*, 3(2):135–176, 2001.

[11] S. Etienne-Manneville and A. Hall. Rho GTPases in cell biology. *Nature*, 420:629–635, 2002.

[12] F. Fages and S. Soliman. From reaction models to influence graphs and back: A theorem. In *FMSB'08*, LNCS 5054, pages 90–102. Springer, 2008.

[13] J. Feret, V. Danos, J. Krivine, R. Harmer, and W. Fontana. Internal coarse-graining of molecular systems. *Proceedings of the National Academy of Sciences*, 106(16):6453–6458, 2008.

[14] A. B. Goryachev and A. V. Pokhilko. Computational model explains high activity and rapid cycling of Rho GTPases within protein complexes. *PLOS Computational Biology*, 2:1511–1521, 2006.

[15] M. L. Guerriero, A. Dudka, N. Underhill, J. K. Heath, and C. Priami. Narrative-based computational modelling of the gp130/jak/stat signalling pathway. *BMC Systems Biology*, 3(40), 2009.

[16] M. Heiner, D. Gilbert, and R. Donaldson. Petri nets for systems and synthetic biology. In *SFM'08*, volume 5016 of *LNCS*, pages 215–264. Springer, 2008.

[17] A. B. Jaffe and A. Hall. Rho GTPases: Biochemistry and biology. *Annual Review of Cell and Developmental Biology*, 21:247–269, 2005.

[18] O. Kahramanoğulları. On linear logic planning and concurrency. *Information and Computation*, 207:1229–1258, 2009.

[19] O. Kahramanoğulları, L. Cardelli, and E. Caron. An intuitive modelling interface for systems biology. In *DCM'09*, volume 9 of *EPTCS*, pages 73–86, 2009.

[20] M. Ajmone Marsan, G. Balbo, G. Conte, S. Donatelli, and G. Franceschinis, editors. *Modelling with Generalized Stochastic Petri Nets*. ACM, 1995.

[21] M. Nielsen, G. Plotkin, and G. Winskel. Event structures and domains, part 1. *Theoretical Computer Science*, 5(3):223–256, 1981.

[22] A. Phillips and L. Cardelli. Efficient, correct simulation of biological processes in stochastic Pi-calculus. In *CMSB'07*, volume 4695 of *LNBI*. Springer, 2007.

[23] C. Priami, P. Quaglia, and A. Romanel. Blenx static and dynamic semantics. In *CONCUR'09*, volume 5710 of *LNCS*, pages 37–52. Springer, 2009.

[24] C. Priami, A. Regev, E. Shapiro, and W. Silverman. Application of a stochastic name-passing calculus to representation and simulation of molecular processes. *Information Processing Letters*, 80:25–31, 2001.

[25] V. Shahrezaei and P. S. Swain. The stochastic nature of biochemical networks. *Current Opinion in Biotechnology*, 19(4):369–374, 2008.

[26] C. Talcott. Pathway logic. In *SFM'08*, volume 5016 of *LNCS*, pages 21–53, 2008.

[27] G. Winskel and M. Nielsen. Models for concurrency. In *Handbook of Logic in Computer Science*, volume 4, pages 1–148. Oxford University Press, 1995.

Appendix A

```
directive sample 4.0
directive plot RD(); R(); RT();
               RDE(); RE(); RTE();
               RDA(); RTA(); RA()

val D = 50.0
val T = 500.0

new a1@1.0:chan()
new a2@1.0:chan()
new a3@1.0:chan()

new e1@0.0054:chan()
new e2@0.0075:chan()
new e3@0.43:chan()


let A() = do ?a1; ()
          or ?a2; ()
          or ?a3; ()

let E() = do ?e1; ()
          or ?e2; ()
          or ?e3; ()

let R(id:int) =  do delay@0.033*D; RD(id)            (* 9 -> 1 *)
                 or delay@0.1*T; RT(id)              (* 9 -> 2 *)
                 or !a3; RA(id)                      (* 9 -> 7 *)
                 or !e3; RE(id)                      (* 9 -> 4 *)

and RD(id:int) = do delay@0.02; R(id)                (* 1 -> 9 *)
                 or !a1; RDA(id)                     (* 1 -> 8 *)
                 or !e1; RDE(id)                     (* 1 -> 3 *)

and RT(id:int) = do delay@0.02; R(id)                (* 2 -> 9 *)
                 or delay@0.02; RD(id)               (* 2 -> 1 *)
                 or !e2; RTE(id)                     (* 2 -> 5 *)
                 or !a2; RTA(id)                     (* 2 -> 6 *)

and RE(id:int) = do delay@0.033*D; RDE(id)           (* 4 -> 3 *)
                 or delay@0.1*T; RTE(id)             (* 4 -> 5 *)
                 or delay@1.074; ( R(id) | E() )     (* 4 -> 9 *)

and RDE(id:int) = do delay@0.136; ( RD(id) | E() )   (* 3 -> 1 *)
```

```
                  or delay@6.0; RE(id)                (* 3 -> 4 *)

and RTE(id:int) = do delay@76.8; ( RT(id) | E() )     (* 5 -> 2 *)
                  or delay@0.02; RDE(id)              (* 5 -> 3 *)
                  or delay@0.02; RE(id)               (* 5 -> 4 *)

and RTA(id:int) = do delay@0.0002; RA(id)             (* 6 -> 7 *)
                  or delay@2104.0; RDA(id)            (* 6 -> 8 *)
                  or delay@3.0; ( RT(id) | A() )      (* 6 -> 2 *)

and RA(id:int) = do delay@0.1*D; RDA(id)              (* 7 -> 8 *)
                 or delay@0.0085*T; RTA(id)           (* 7 -> 6 *)
                 or delay@500.0; ( R(id) | A() )      (* 7 -> 9 *)

and RDA(id:int) = do delay@500.0; ( RD(id) | A() )    (* 8 -> 1 *)
                  or delay@0.02; RA(id)               (* 8 -> 7 *)

let ProduceR(id:int) = if id < 1001
                 then (R(id) | ProduceR(id+1) )
                 else()

run 776 of E()
run 1 of A()
run 1 of ProduceR(1)
```

Appendix B

The flux analysis output for the simulation with $R_0 = 1000$, $E_0 = 776$ and $A_0 = 1$, for the time interval $2.0 < t < 2.5$.

```
Reactions:
----------

1: A R  --> RA  fires 0 times.
2: RA  --> A R  fires 0 times.
3: RTA  --> A RT  fires 0 times.
4: R  --> RD  fires 0 times.
5: RD  --> R  fires 0 times.
6: R  --> RT  fires 0 times.
7: RTE  --> RDE  fires 1 times.
8: RE  --> RDE  fires 2 times.
9: RT  --> RD  fires 9 times.
10: RDE  --> E RD  fires 3 times.
11: RE  --> E R  fires 2 times.
12: E R  --> RE  fires 7 times.
13: RTE  --> RE  fires 2 times.
14: A RD  --> RDA  fires 16 times.
15: A RT  --> RTA  fires 126 times.
16: RTA  --> RDA  fires 126 times.
17: E RD  --> RDE  fires 132 times.
18: RDA  --> A RD  fires 142 times.
19: RT  --> R  fires 6 times.
20: RDE  --> RE  fires 149 times.
21: RE  --> RTE  fires 145 times.
22: RTE  --> E RT  fires 2240 times.
23: E RT  --> RTE  fires 2095 times.


Extracted dependencies:
-----------------------

6 ==> 23  appears 2 times.
7 ==> 20  appears 1 times.
8 ==> 20  appears 3 times.
9 ==> 14  appears 1 times.
9 ==> 17  appears 5 times.
10 ==> 17  appears 2 times.
11 ==> 12  appears 2 times.
12 ==> 21  appears 4 times.
13 ==> 21  appears 1 times.
14 ==> 18  appears 16 times.
15 ==> 16  appears 126 times.
16 ==> 18  appears 126 times.
17 ==> 10  appears 3 times.
17 ==> 20  appears 145 times.
18 ==> 14  appears 15 times.
18 ==> 17  appears 125 times.
19 ==> 12  appears 5 times.
20 ==> 8  appears 2 times.
20 ==> 11  appears 2 times.
20 ==> 21  appears 140 times.
21 ==> 13  appears 1 times.
21 ==> 22  appears 148 times.
22 ==> 9  appears 9 times.
22 ==> 15  appears 126 times.
22 ==> 19  appears 6 times.
22 ==> 23  appears 2093 times.
23 ==> 7  appears 1 times.
23 ==> 13  appears 1 times.
23 ==> 22  appears 2092 times.

================================
================================
```

The flux analysis output for the simulation with $R_0 = 1000$, $E_0 = 776$ and $A_0 = 10$, for the time interval $1.7 < t < 1.8$.

```
Reactions:
----------

1: RA  --> RDA  fires 0 times.
2: RTE  --> RDE  fires 0 times.
3: RTA  --> A RT  fires 0 times.
4: R  --> RD  fires 0 times.
5: RTE  --> RE  fires 0 times.
6: RT  --> RD  fires 0 times.
7: RDE  --> E RD  fires 0 times.
8: RD  --> R  fires 2 times.
9: A R  --> RA  fires 1 times.
10: RA  --> A R  fires 1 times.
11: E R  --> RE  fires 10 times.
12: RE  --> RDE  fires 3 times.
13: RT  --> R  fires 1 times.
14: R  --> RT  fires 2 times.
15: RE  --> E R  fires 10 times.
16: RTA  --> RDA  fires 101 times.
17: A RT  --> RTA  fires 101 times.
18: A RD  --> RDA  fires 157 times.
19: E RD  --> RDE  fires 123 times.
20: RTE  --> E RT  fires 255 times.
21: RDE  --> RE  fires 137 times.
22: E RT  --> RTE  fires 134 times.
23: RDA  --> A RD  fires 261 times.
24: RE  --> RTE  fires 139 times.


Extracted dependencies:
-----------------------

7 ==> 18  appears 1 times.
7 ==> 19  appears 1 times.
8 ==> 9  appears 1 times.
```

```
8 ==> 14  appears 1 times.
9 ==> 10  appears 1 times.
10 ==> 11  appears 1 times.
11 ==> 24  appears 13 times.
12 ==> 21  appears 5 times.
13 ==> 14  appears 1 times.
15 ==> 11  appears 9 times.
16 ==> 23  appears 102 times.
17 ==> 16  appears 101 times.
18 ==> 23  appears 159 times.
19 ==> 21  appears 132 times.
20 ==> 13  appears 1 times.
20 ==> 17  appears 101 times.
20 ==> 22  appears 134 times.
21 ==> 12  appears 3 times.
21 ==> 15  appears 10 times.
21 ==> 24  appears 126 times.
22 ==> 20  appears 117 times.
23 ==> 8  appears 2 times.
23 ==> 18  appears 156 times.
23 ==> 19  appears 122 times.
24 ==> 20  appears 138 times.

==================================
==================================
```

The flux analysis output for the simulation with $R_0 = 1000$, $E_0 = 776$ and $A_0 = 100$, for the time interval $0.3 < t < 0.4$.

```
Reactions:
----------

1: RA  --> RTA  fires 0 times.
2: RA  --> RDA  fires 0 times.
3: R  --> RD  fires 0 times.
4: A R  --> RA  fires 0 times.
5: RTA  --> A RT  fires 0 times.
6: R  --> RT  fires 0 times.
7: RT  --> RD  fires 0 times.
8: RDA  --> RA  fires 1 times.
9: RE  --> E R  fires 1 times.
10: RA  --> A R  fires 1 times.
11: RD  --> R  fires 2 times.
12: E R  --> RE  fires 4 times.
13: RE  --> RDE  fires 4 times.
14: RDE  --> E RD  fires 6 times.
15: E RT  --> RTE  fires 22 times.
16: E RD  --> RDE  fires 157 times.
17: RDE  --> RE  fires 143 times.
18: A RT  --> RTA  fires 148 times.
19: RTA  --> RDA  fires 149 times.
20: RE  --> RTE  fires 140 times.
21: RTE  --> E RT  fires 168 times.
22: A RD  --> RDA  fires 2606 times.
23: RDA  --> A RD  fires 2756 times.


Extracted dependencies:
-----------------------

8 ==> 10  appears 1 times.
9 ==> 12  appears 1 times.
10 ==> 12  appears 1 times.
11 ==> 12  appears 2 times.
12 ==> 20  appears 6 times.
13 ==> 17  appears 2 times.
14 ==> 22  appears 6 times.
15 ==> 21  appears 22 times.
16 ==> 14  appears 6 times.
16 ==> 17  appears 141 times.
17 ==> 9  appears 1 times.
17 ==> 13  appears 4 times.
17 ==> 20  appears 134 times.
18 ==> 19  appears 149 times.
19 ==> 23  appears 151 times.
20 ==> 21  appears 146 times.
21 ==> 15  appears 22 times.
21 ==> 18  appears 148 times.
22 ==> 8  appears 1 times.
22 ==> 23  appears 2605 times.
23 ==> 11  appears 2 times.
23 ==> 16  appears 157 times.
23 ==> 22  appears 2600 times.

==================================
==================================
```